

YOUNG STARS: IRREGULARITIES OF THE VELOCITY FIELD

J. Torra¹, A. E. Gómez², F. Figueras¹, F. Comerón³,
S. Grenier², M.O. Mennessier⁴, M. Mestres¹, D. Fernández¹

¹Departament d'Astronomia i Meteorologia. Universitat de Barcelona, Spain

²Observatoire de Paris-Meudon, D.A.S.G.A.L., France

³European Southern Observatory, Garching bei München, Germany

⁴GRAAL. Université de Montpellier II, France

ABSTRACT

We present here a first review of the structure and kinematics of the local system of young stars. Hipparcos astrometric data for a large sample of O and B stars have been complemented with a careful compilation of available radial velocities and Strömgren photometry thus providing reliable distance, spatial velocity and age for each star in the sample. The fundamental parameters characterizing the structure of the Gould Belt, inclination, size and age are determined. The velocity field is studied by means of the classical first order approach. Oort's constants A, B, C, K are determined for several subsamples selected by age and the results explained by the presence of the Gould Belt.

Key words: galactic kinematics; young stars; Gould Belt.

1. INTRODUCTION

O and B stars in the solar neighbourhood have been traditionally used as probes of galactic structure and kinematics. Their intrinsic brightness allows their observations to great distances from the Sun, and due to their youth, their motions can be expected to hold important clues to the processes that formed them. An important characteristic of the distribution of young stars were recognized more than one century ago when J. Herschel realized that the local system of young stars shows a concentration of stars along a great circle tilted respect to the galactic equator. Since the pioneering work by Gould in 1874-1879 a great number of studies have been devoted to the Gould Belt trying to explain its structure and kinematics, characterized by the existence of an expanding motion (Lesh 1968, Stothers & Frogel, 1974, Frogel & Stothers 1977). More recently Westin (1985), Comerón et al. (1991), Comerón (1992), Palouš (1995) and Lindblad et al. (1997) have studied the Belt and determined its orientation, age and kinematics. Several models have been presented in order to explain the origin of the Gould Belt: it has been

interpreted as a local effect of the spiral arm (Lindblad 1973), by energetic event on the galactic disk (Olano 1982, Elmegreen 1982), corrugation waves in the galactic disk (Nelson 1976) or by an halo-disk interaction (Comerón 1992, Lepine & Duvert 1995).

The velocity field of young stars is described to first order by the Oort's formulae (Ogorodnikov 1965) relating the observed radial velocity, distance and proper motion with the solar motion and the gradients of the velocity field. Several works have been devoted to the determination of the Oort's constants considering only differential rotation or including other effects such as spiral structure or expanding motions (Lindblad 1980, Crézé et al. 1973, Byl et al. 1981, Comerón et al. 1991 among others).

2. THE CATALOGUE

Our initial sample contains 6922 O-B type stars (*Hipparcos Internal proposal, INCA060*), of which 5846 belong to the Hipparcos *Survey*. The sources of radial velocities have been the Barbier-Brossat (1997) and the Duflo et al. (1995) compilations. Priority has been given to the first one, and only stars with quality A, B or C in the last compilation have been considered (Grenier 1997). Using these sources, only 3182 stars of our total sample have known radial velocity, this parameter being, at present, the most important limitation to undertake the study of the velocity field in the solar neighbourhood.

Strömgren photometry has been used to compute photometric distances and ages. 3031 stars from our sample have complete photometry in the Hauck & Mermilliod (1996) catalogue. From these, we have rejected the stars being double or multiple from Hipparcos ($\rho < 10$ arcsec and $\Delta m < 3$ mag), the variable stars ($\Delta m > 0.6$ mag) and the stars showing peculiarities in the spectral type or in the photometric indices (Masana 1994). Crawford (1978) calibration has been used to derive photometric distances which are compared to the Hipparcos distances – computed as the inverse of the parallax – in Figure 1. Although no systematic trend seems to be present, an expected large scattering is observed for stars at distances higher than 200 pc. Other photometric cal-

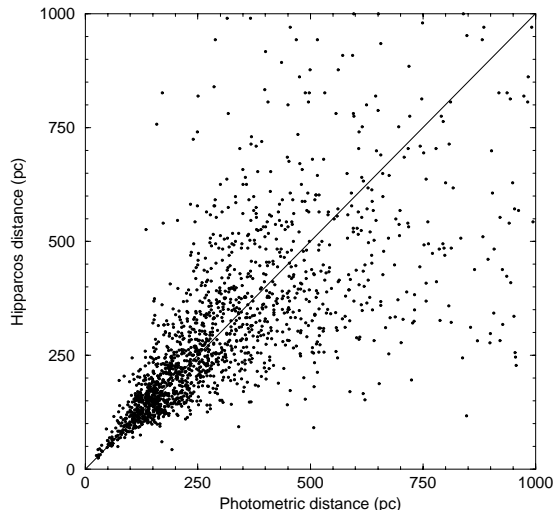


Figure 1. Comparison between photometric and Hipparcos distances for the working sample (2139 stars). Photometric distances computed from Crawford (1978) calibrations.

ibrations (Balona et al. 1984, Jakobsen 1985) have been also considered for the computation of photometric distances, thus checking that the kinematic results do not depend of the calibration used.

Individual ages have been computed from the evolutionary models of Bressan et al. (1993) for solar composition following Asiain et al. (1997) interpolation algorithm, which considers, as input parameters, the T_{eff} and $\log g$ derived from the photometric indices (Moon et al. 1985, grids). The stars showing a relative error on age larger than 100 per cent have been rejected (these are stars near or below the ZAMS for which the obtained age is not reliable). The histograms of the age distribution and the computed individual errors are presented in Figure 2 and Figure 3 respectively.

According to the physical information available we have defined two working samples:

- Sample 1: 2139 stars with good ($\Delta\tau/\tau \leq 100$ per cent) ages and photometric distances. Useful to determine the fundamental parameters of the Gould Belt.
- Sample 2: 1539 stars, a subsample of Sample 1, containing the stars with known radial velocities having $\epsilon_{V_r} \leq 7$ km/s, well suited for the analysis of the systematic velocity field.

3. FUNDAMENTAL PARAMETERS OF THE GOULD BELT

We can see in Figure 4 where (X,Y,Z) are the galactic heliocentric coordinates with X directed towards the galactic center, Y in the direction of the galactic rotation and Z directed towards the north galactic pole, the well known spatial distribution of young

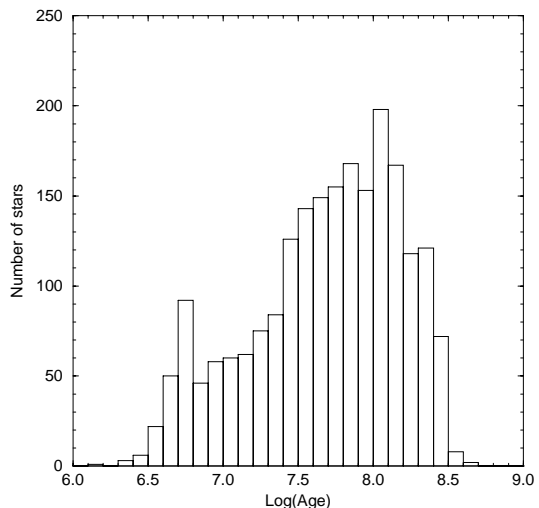


Figure 2. Age distribution of the working sample (2139 stars). Ages computed from Bressan et al. (1993) evolutionary models.

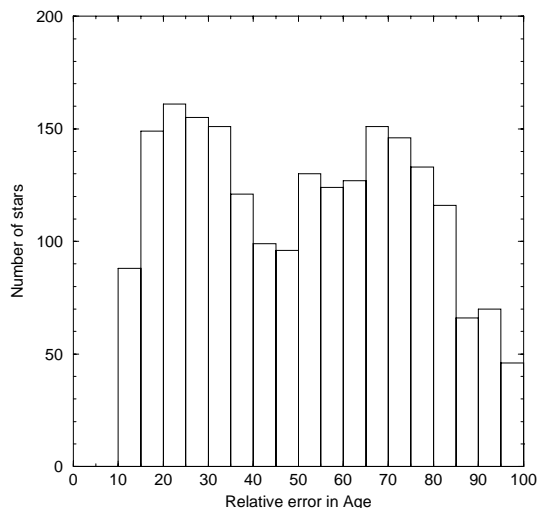


Figure 3. Distribution of the relative errors in age (2139 stars).

stars clearly showing the galactic belt and the inclined and assymmetric structure of the Gould Belt.

We have not tried to individually separate the stars belonging to the Gould Belt from the ones in the galactic plane; otherwise we will follow the method developed by Comerón et al. (1994), well suited for large samples, which allows a statistical determination of the parameters characterizing the geometry of both belts. We assume that the density distribution of the sample in the celestial sphere can be written as:

$$\sigma(l, b) = \sigma_G(l, b) + \sigma_g(l, b) \quad (1)$$

where σ_G and σ_g are the density distributions around the Gould Belt and the galactic equator respectively. For each one of these distributions we assume that:

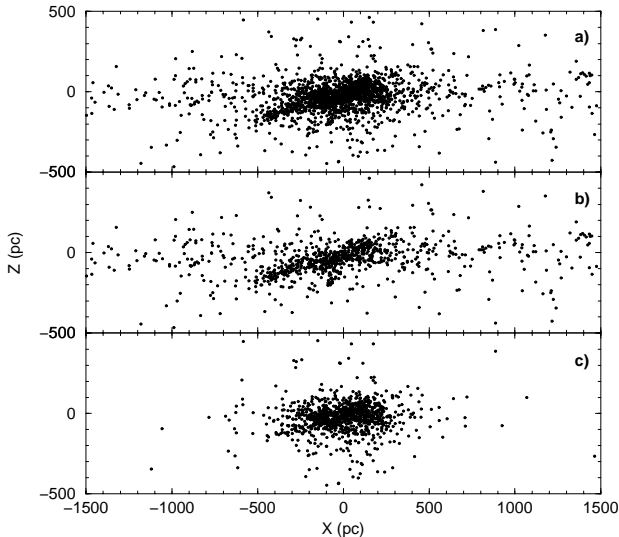


Figure 4. Spatial distribution in the (X, Z) plane: (a) total sample of 2139 stars; (b) 1120 stars with $\tau \leq 60$ Myr; (c) 1019 stars with $\tau > 60$ Myr.

$$\sigma(\theta) \propto \exp\left(-\frac{\sin^2 \theta}{2 \sin^2(\xi/2)}\right) \quad (2)$$

θ being the angular distance to the equator of the corresponding distribution and ξ its halfwidth. The geometric parameters: inclination, i , longitude of the ascending node, Ω , halfwidths of both belts ξ_G, ξ_g as well as the fraction of the stars, q , belonging to the Gould Belt which enters in the proportionality constant in Equation 2 are determined by an iterative maximum likelihood method.

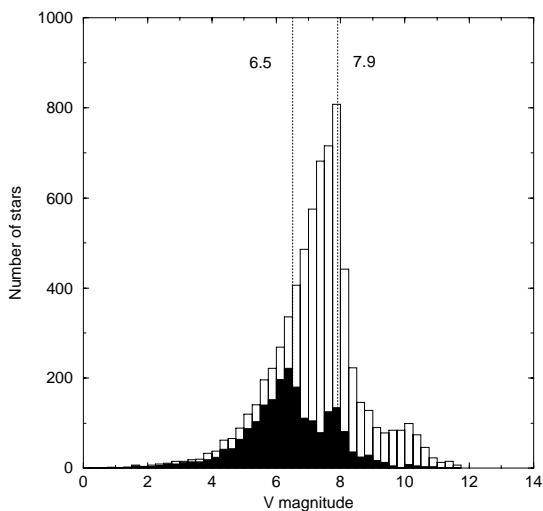


Figure 5. Distribution of apparent magnitudes: 6922 stars from INCA060 proposal (empty histogram) and 2139 stars with good ages and photometric distances (filled histogram).

The method has the advantage that the heliocentric distance of the stars are only used to define the limit of the subsamples considered. The method will produce accurate results only if the sample is complete enough. As can be seen in Figure 5, if we want to use

individual ages, to be complete, our sample is limited to stars brighter than 6.5 mag.

In Table 1 we show the results obtained for several subsamples of sample 1 selected by age and photometric distance. Assuming $q > 0$ as an indicator of the presence of the Gould Belt, we see that it is defined by $i = 17^\circ - 20^\circ$ and $\Omega = 278^\circ - 290^\circ$, in good agreement with previous results. We found the highest q value, 0.94, for stars younger than 30 million years and distances between 400 and 600 pc; some older stars up to 60 million years establish the limits of the Gould Belt at 400 pc, and very few, if any, stars older than 60 million years indicate also a limit of 400 pc. Tsoumis & Fricke (1979) considered the extent to be 450–600 pc, and Westin (1985) considered 250–500 pc depending on the galactic longitude. In Figure 4 we can see the relationship between age and structure in the X, Z plane. We want to remark that when the method is applied to the complete sample of OB Survey stars with $V \leq 7.9$ (see Figure 5) the same conclusions are reached, although in this case only spectral types are available as indicators of evolution.

4. SYSTEMATIC MOTION OF YOUNG STARS

4.1. Distribution of Residual Velocities

The sample of 1539 O-B type stars used to derive the systematic motion of young stars in the solar neighbourhood shows (see Figure 6) an irregular distribution in the (U, V) plane, (U, V, W) being the components of the velocity in the system defined in Section 3. The sample is reduced to 1417 stars when those with residual velocity exceeding 65 km s^{-1} are eliminated. Mean velocity and dispersions of the working sample are:

$$(U_o, V_o, W_o) = (-12.7, -14.6, -8.1) \text{ km s}^{-1}$$

$$(\sigma_U, \sigma_V, \sigma_W) = (16.0, 11.5, 8.0) \text{ km s}^{-1}$$

The values obtained for the solar motion when age groups are considered (see Table 2) are affected

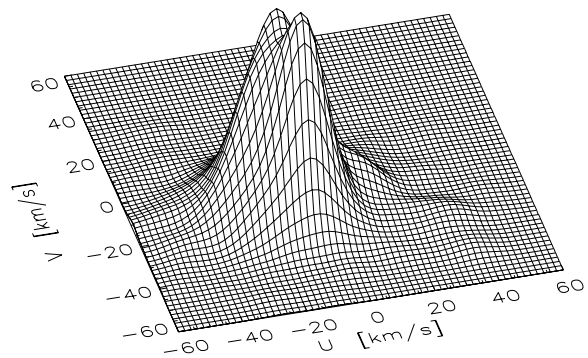


Figure 6. (U, V) distribution of the 1539 stars with good kinematical data.

Table 1. Geometrical parameters of the Gould Belt as a function of distance and age: inclination (i_G), longitude of the ascending node (Ω_G), fraction of stars belonging to the Gould Belt (q), angular width of the Gould Belt (ξ_G) and the galactic belt (ξ_g), and number of stars (N).

ρ (pc)	i_G ($^\circ$)	Ω_G ($^\circ$)	q	ξ_G ($^\circ$)	ξ_g ($^\circ$)	N
0-30 10^6 years						
$r < 400$	19.9 ± 8.2	278.0 ± 41.9	0.86 ± 0.03	14.17	10.91	103
$400 \leq r < 600$	17.6 ± 15.2	287.8 ± 62.4	0.94 ± 0.03	10.06	11.79	56
$600 \leq r < 800$	13.5 ± 4.0	301.4 ± 13.8	0.50 ± 0.09	15.37	9.19	31
$600 \leq r < 2000$	13.9 ± 4.8	322.0 ± 21.9				91
30-60 10^6 years						
$r < 400$	20.8 ± 10.3	290.4 ± 25.2	0.65 ± 0.03	8.43	23.39	201
$400 \leq r < 600$	9.5 ± 2.1	283.8 ± 5.5				37
$600 \leq r < 800$	13.7 ± 5.4	283.7 ± 8.9	0.19 ± 0.13	43.57	6.99	9
$600 \leq r < 2000$	18.5 ± 9.5	282.3 ± 10.9	0.46 ± 0.09	28.32	6.25	31
≥ 60 10^6 years						
$r < 400$	24.0 ± 11.5	278.8 ± 31.7	0.35 ± 0.02	23.92	20.35	596
$400 \leq r < 600$	21.2 ± 5.2	178.3 ± 20.3				20

by the presence of moving groups as described by Figueras et al. (1997).

Thanks to the good quality of the Hipparcos astrometric data and the accurate compilation of radial velocities, the mean errors are $(\epsilon_U, \epsilon_V, \epsilon_W) = (3.8, 3.8, 3.0)$ km s $^{-1}$, between 1 and 2 km s $^{-1}$ better than previous studies.

4.2. Derivation of the Oort's Constants

The Oort's constants have been derived using a first-order approximation of the systematic velocity field (Ogorodnikov 1965):

$$V_r = Ar \sin 2l \cos^2 b + Cr \cos 2l \cos^2 b + Kr \cos^2 b - U_\odot \cos l \cos b - V_\odot \sin l \cos b - W_\odot \sin b \quad (3)$$

$$rk\mu_l \cos b = Ar \cos 2l \cos b + Br \cos b - Cr \sin 2l \cos b + U_\odot \sin l - V_\odot \cos l \quad (4)$$

$$rk\mu_b = -Ar \sin 2l \sin b \cos b - Cr \cos 2l \sin b \cos b - Kr \sin b \cos b + U_\odot \cos l \sin b + V_\odot \sin l \sin b - W_\odot \cos b \quad (5)$$

where l, b are the galactic coordinates, r the distance, V_r the radial velocity, μ_l and μ_b the proper motions. U_\odot, v_\odot and W_\odot are the components of the peculiar motion of the Sun in km s $^{-1}$ respect to the circular velocity and A, B, C and K are the Oort's constants, linear combinations of the gradients of the systematic velocity:

$$A = \frac{1}{2} \left(\frac{\partial U}{\partial y} + \frac{\partial V}{\partial x} \right)$$

$$B = -\frac{1}{2} \left(\frac{\partial U}{\partial y} - \frac{\partial V}{\partial x} \right)$$

$$C = \frac{1}{2} \left(\frac{\partial U}{\partial x} - \frac{\partial V}{\partial y} \right)$$

$$K = \frac{1}{2} \left(\frac{\partial U}{\partial x} + \frac{\partial V}{\partial y} \right)$$

where no systematic motion perpendicular to the plane is considered other than that arising from the solar peculiar motion. The conversion factor $k = 4.74$ if velocities are expressed in km/s, proper motions in arcsec/yr, and distances in parsecs.

The three equations – radial velocity and proper motion in longitude and latitude – have been simultaneously solved using an unweighted least square fit. In Table 2 we show the results obtained when different subsamples selected in distance and age are considered. The results for stars with distances $70 \leq r < 400$ pc are summarized in Figure 7 where we can appreciate the monotonic behaviour of the A and B Oort's constants against age. The classical values of $A \sim 15$ and $B \sim -12$ km s $^{-1}$ kpc $^{-1}$ are obtained for the oldest sample, while values as low as $A = 0$ km s $^{-1}$ kpc $^{-1}$ and $B = -26$ km s $^{-1}$ kpc $^{-1}$ are found for the youngest stars. The K term shows, as expected, a strong decrease with increasing age and disappears for ages between 40 and 60 million years, thus confirming its relationship with the expanding motion of the Gould Belt. On the contrary, the C constant shows a rather erratic and not explained behaviour that could be related to the spiral arms. The same trends appear in Figure 8 where we have plotted, for broad age groups, the values of the Oort's constants against the distance. We see that for the youngest age group A and B take low values for the nearest region associated with the Gould Belt, reaching the classical values for distant stars, whereas for the oldest group quite stable classical values are found. The K constant reaches the zero values at a distance of about 500 pc which could indicate the extend of the Belt in agreement with the determination we did in the previous paragraph. Now again the C constant behaves rather different being the intermediate group (30–60 Myr) the one showing the maximum variation.

Table 2. Oort's constants and residual solar motion as a function of distance and age. Units: A, B, C, K in $\text{km s}^{-1} \text{kpc}^{-1}$; $U_{\odot}, V_{\odot}, W_{\odot}$ in km s^{-1} .

Age (10^7 yrs)	A	B	C	K	U_{\odot}	V_{\odot}	W_{\odot}	N
$70 \text{ pc} \leq r < 400 \text{ pc}$								
< 2	-0.4 ± 4.6	-26.0 ± 4.6	3.1 ± 4.6	14.3 ± 4.6	10.2 ± 1.1	17.9 ± 1.1	7.6 ± 1.0	57
$2 \leq E < 4$	7.5 ± 2.8	-17.4 ± 2.8	9.0 ± 2.8	10.1 ± 2.8	10.1 ± 0.7	16.5 ± 0.7	8.0 ± 0.6	114
$4 \leq E < 6$	7.1 ± 3.2	-15.1 ± 3.2	6.8 ± 3.2	3.8 ± 3.2	13.4 ± 0.7	15.3 ± 0.7	7.7 ± 0.7	134
$6 \leq E < 8$	12.0 ± 3.4	-13.6 ± 3.4	7.5 ± 3.4	-1.1 ± 3.4	12.6 ± 0.8	15.7 ± 0.8	7.6 ± 0.7	107
$8 \leq E < 10$	14.1 ± 4.0	-12.2 ± 4.0	2.0 ± 4.0	-1.5 ± 4.0	14.6 ± 0.9	15.0 ± 0.9	7.7 ± 0.9	94
< 3	3.7 ± 3.1	-22.6 ± 3.1	3.7 ± 3.1	16.1 ± 3.1	10.4 ± 0.7	17.2 ± 0.7	8.1 ± 0.7	107
$3 \leq E < 6$	6.9 ± 2.4	-15.5 ± 2.4	8.6 ± 2.4	4.1 ± 2.4	12.3 ± 0.6	15.7 ± 0.6	7.6 ± 0.5	198
≥ 6	13.7 ± 1.9	-9.8 ± 1.9	-3.7 ± 1.9	-0.2 ± 1.9	12.4 ± 0.4	14.4 ± 0.4	7.2 ± 0.2	625
$400 \text{ pc} \leq r < 800 \text{ pc}$								
< 2	14.1 ± 2.1	-21.2 ± 2.1	1.3 ± 2.1	-2.4 ± 2.1	9.7 ± 1.2	15.4 ± 1.2	6.5 ± 1.1	73
$2 \leq E < 4$	9.5 ± 2.0	-23.8 ± 2.0	-1.3 ± 2.0	-0.9 ± 2.0	9.1 ± 1.1	13.9 ± 1.1	9.7 ± 0.9	78
$4 \leq E < 6$	-0.1 ± 3.2	-15.1 ± 3.2	-1.4 ± 3.2	0.7 ± 3.2	17.3 ± 1.6	13.3 ± 1.6	7.8 ± 1.5	45
$6 \leq E < 8$	15.0 ± 4.4	-10.9 ± 4.4	2.5 ± 4.4	-9.7 ± 4.4	13.7 ± 2.3	13.7 ± 2.3	10.4 ± 2.2	26
< 3	12.5 ± 1.7	-21.4 ± 1.7	-0.4 ± 1.7	-3.9 ± 1.7	9.9 ± 1.0	14.9 ± 1.0	7.5 ± 0.8	117
$3 \leq E < 6$	4.7 ± 2.2	-18.6 ± 2.2	0.1 ± 2.2	2.8 ± 2.2	14.0 ± 1.2	13.4 ± 1.2	9.2 ± 1.1	79
≥ 6	11.9 ± 3.6	-8.3 ± 3.6	-2.0 ± 3.6	-6.9 ± 3.6	12.6 ± 1.8	12.1 ± 1.8	8.6 ± 1.7	49
$400 \text{ pc} \leq r < 1500 \text{ pc}$								
< 2	14.5 ± 1.1	-14.9 ± 1.1	-0.4 ± 1.1	-4.0 ± 1.1	10.6 ± 1.0	14.3 ± 1.0	7.8 ± 1.0	136
$2 \leq E < 4$	10.2 ± 1.6	-18.1 ± 1.6	-1.2 ± 1.6	-1.1 ± 1.6	9.4 ± 1.2	13.0 ± 1.2	9.5 ± 1.0	107
$4 \leq E < 6$	2.5 ± 2.3	-13.5 ± 2.3	-5.7 ± 2.3	0.5 ± 2.3	18.7 ± 1.5	12.5 ± 1.5	9.5 ± 1.4	61
$6 \leq E < 8$	11.6 ± 4.3	-11.7 ± 4.3	0.3 ± 4.3	-8.3 ± 4.3	11.4 ± 2.4	15.8 ± 2.4	9.0 ± 2.3	30
< 3	14.1 ± 1.0	-14.8 ± 1.0	-0.6 ± 1.0	-4.3 ± 1.0	10.2 ± 0.8	13.8 ± 0.8	8.1 ± 0.8	191
$3 \leq E < 6$	4.5 ± 1.6	-16.0 ± 1.6	-3.0 ± 1.6	0.3 ± 1.6	15.5 ± 1.2	12.9 ± 1.2	9.9 ± 1.1	113
≥ 6	10.2 ± 3.3	-10.2 ± 3.3	-1.9 ± 3.3	-6.7 ± 3.3	10.7 ± 1.8	14.1 ± 1.8	7.2 ± 1.8	55

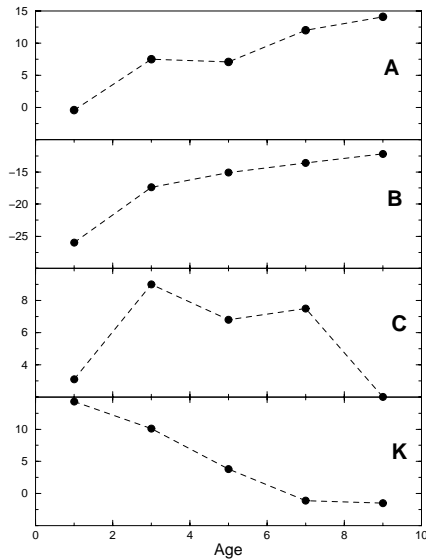


Figure 7. Variation of A, B, C, K Oort's constants against age for stars within $70 \text{ pc} \leq r < 400 \text{ pc}$. (Units: 10^7 yr and $\text{km s}^{-1} \text{kpc}^{-1}$)

ACKNOWLEDGEMENTS

This work has been supported by CICYT (ESP95-180), PICASSO program and PICS-348.

REFERENCES

Asiain, R., Torra, J., Figueras, F. 1997, A&A, (in press)

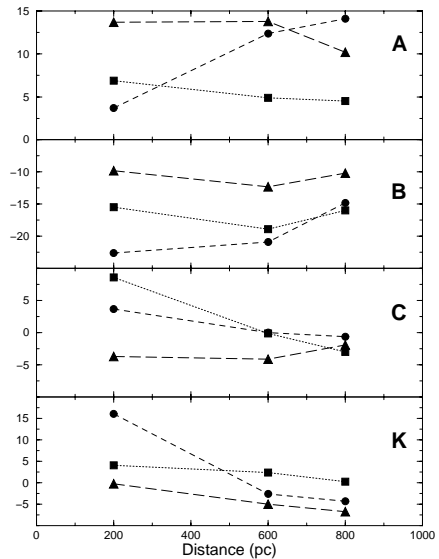


Figure 8. Variation of A, B, C, K Oort's constants against distance. Dots: stars with ages between 0-30 Myr; squares: ages between 30-60 Myr and triangles: ages larger than 60 Myr. (Units: $\text{km s}^{-1} \text{kpc}^{-1}$).

Balona, L.A., Shobbrook, R.R. 1984, MNRAS 211, 973

Barbier-Brossat, M. 1997, private communication

Bressan, A., Fagotto, F., Bertelli, G., Chiosi, C. 1993, A&AS 100, 647

Byl, J., Ovtenden, M.W. 1981, MNRAS 196, 659

Comerón, F., Torra, J. 1991, A&A 241, 57

Comerón, F. 1992, PhD Thesis, Universitat de Barcelona, Spain

- Comerón, F., Torra, J., Gómez, A.E. 1994, A&A 286, 789
- Crawford, D.L. 1979, AJ 83, 48
- Crézé, M., Mennessier, M.O. 1973, A&A 27, 281
- Dufflot, M., Figon, P., Meyssonier, N. 1995, A&AS 114, 269
- Elmegreen, G.B. 1982, in The formation of giant cloud complexes, Cambridge Univ. Press
- Figueras, F., Asiain, R., Chen, B., Comerón, F., Gómez, A.E., Grenier, S., Lebreton, Y., Moreno, M., Sabas, V. 1997, this volume
- Frogel, J.A., Stothers, R. 1977, AJ 81, 890
- Grenier, S. 1997, private communication
- Hauck, B., Mermilliod, J.C. 1996, private communication
- Jakobsen, A.M. 1985, PhD Thesis, University of Aarhus, Denmark
- Lesh, J.R. 1968, ApJS 151, 371
- Lepine, J., Duvert, G. 1994, A&A 286, 60
- Lindblad, P.O., Grape, K., Sandqvist, Aa., Schober, J. 1973, A&A 24, 309
- Lindblad, P.O. 1980, Mitt. Astron. Ges. 48, 151
- Lindblad, P.O., Palouš, J., Lodén, K., Lindegren, L. 1997, this volume
- Masana, E. 1994, Degree of Physics, Universitat de Barcelona, Spain
- Moon, T.T., Dworetzky, M.M. 1985, MNRAS 217, 305
- Nelson, A.H. 1976, MNRAS 177, 265
- Ogorodnikov, K.F. 1965, Dynamic of Stellar Systems, Pergamon Press, Oxford
- Olano, C.A. 1982, A&A 112, 195
- Palouš, J. 1995, Structure and Evolution of Stellar Systems, Ed. V.V. Orlov, in press
- Tsioumis, A., Fricke, W. 1979, A&A 75, 1
- Westin, T.N.G. 1985, A&AS 60, 99